

Resonances in the Total Cross Sections for Metastable Excitation of Noble Gases by Electron Impact

F. M. J. PICHANICK† AND J. AROL SIMPSON
 National Bureau of Standards, Washington, D. C. 20234
 (Received 30 November 1967)

Total cross sections for excitation by electron impact of metastable states in the noble gases helium, neon, argon, krypton, and xenon have been measured as a function of impact energies. A 180° spherical monochromator was used to obtain incident beams of electrons with energy resolutions between 0.035 and 0.050 eV. Metastable atoms were detected in the scattering chamber by electron ejection from a metal surface. The detector was biased negatively to repel scattered electrons, and was electrostatically shielded from the incident electron beam. The cross sections were measured for impact energies up to 5 eV above the metastable thresholds. Several narrow resonances associated with negative-ion states were observed, and where possible their shapes and positions on the energy scale were compared with similar results obtained by different techniques.

1. INTRODUCTION

RESONANCES in the cross sections near inelastic thresholds are an important aspect of electron-atom scattering at low energies. These effects have been strikingly demonstrated¹⁻³ in the electron-helium case by observing the electrons scattered out of a monoenergetic incident beam into elastic and inelastic channels of the differential cross section. This method has not been applied successfully to resonances in inelastic channels for noble gases other than helium. We report here observations of resonances in the total cross sections for metastable excitation of noble gases by electrons. The results show that these resonances, presumably arising from negative-ion states,⁴ play a major role in the cross sections at energies up to 5 eV above threshold. Their predominance is particularly striking in the case of neon, where the structure near 18.5 eV had been previously interpreted in terms of the opening up of inelastic channels.⁵

2. APPARATUS

A well-collimated beam of monoenergetic electrons entered a scattering chamber containing a noble gas at a pressure of up to 0.1 Torr. The energy of the incident electrons with respect to the gas was slowly varied, and the total yield of metastable noble-gas atoms was plotted as a function of this impact energy. The resultant excitation curves gave the variation with impact energy of the total cross section for metastable excitation by electrons.

The electron-scattering spectrometer used in this

experiment has been described elsewhere^{6,7} and is illustrated schematically in Fig. 1. The spectrometer consists of an electron source, a 180° spherical deflector (monochromator), a scattering chamber (gas cell), a second spherical deflector (analyzer), and a Faraday-cup electron detector. The monochromator and analyzer are energy selectors, respectively, for electrons entering and leaving the gas cell. The only major modification of the apparatus involved the gas cell, into which was incorporated a detector for metastable atoms. This is illustrated in Figs. 1 and 2. The gas cell was a 2.2-in.-diam×0.65-in. cylindrical "pillbox" with the incident electron beam running along its axis. Within the cell and concentric with its axis was a 0.9-in.-diam×0.5-in. cylinder (the "grid") made of stainless-steel mesh, which was 50% transparent with 0.02×0.02-in. apertures. The entrance and exit apertures of the gas cell were 0.02-in.-diam holes in 1-in.-diam molybdenum disks. The mounts for these disks also served to hold the grid. The metastable detector itself was a ring suspended outside the grid and concentric with it. The ring, made of 0.006-in. gold foil, was 0.2 in. wide and about 1.3 in. in diam, and was biased negatively with respect to the gas cell by 10–25 V, the magnitude depending on the particular gas target. The purpose of the bias was to prevent elastically scattered electrons from reaching the ring and thereby swamping the metastable current. A fraction of the metastable atoms reaching the ring resulted in the ejection of Auger⁸ electrons, yielding a positive current in the electrometer circuit. This current would have been indistinguishable from that due to positive ions reaching the ring, and for this reason no data were taken above ionization thresholds.

The purpose of the grid was to shield the scattering region from the biasing potential, which otherwise would have produced serious field inhomogeneities along the electron beam. The shielding provided by the grid

† Guest Worker, National Bureau of Standards, 1966–1967. Present address: Sloane Laboratory, Yale University, New Haven, Conn. 06520.

¹ G. J. Schulz and J. W. Philbrick, *Phys. Rev. Letters* **13**, 477 (1964).

² G. E. Chamberlain, *Phys. Rev. Letters* **14**, 581 (1965); G. E. Chamberlain and H. G. M. Heideman, *ibid.* **15**, 337 (1965).

³ G. E. Chamberlain, *Phys. Rev.* **155**, 46 (1967).
⁴ E. Baranger and E. Gerjuoy, *Phys. Rev. Letters* **106**, 1182 (1957); J. Arol Simpson and U. Fano, *ibid.* **11**, 158 (1963).

⁵ J. Olmsted, III, A. S. Newton, and K. Street, Jr., *J. Chem. Phys.* **42**, 2321 (1965).

⁶ J. Arol Simpson, *Rev. Sci. Instr.* **35**, 1698 (1964).

⁷ C. E. Kuyatt, J. Arol Simpson, and S. R. Mielczarek, *Phys. Rev.* **138**, A385 (1965).

⁸ R. Dorrenstein, *Physica* **9**, 447 (1942); H. D. Hagstrum, *Phys. Rev.* **96**, 336 (1954).

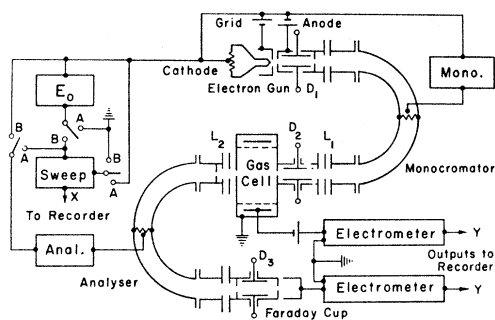


FIG. 1. Schematic illustration of the electron monochromator, gas cell, and associated electronics.

enabled the attainment of an energy resolution of 0.05 eV or better in the incident electron beam.

The current obtained due to metastable atoms ranged from 10^{-9} A for helium (20-eV impact energy) to 10^{-11} A for krypton (10-eV impact energy). These were obtained at energy resolutions of 0.05 eV and at target-gas pressures between 5×10^{-2} and 2×10^{-1} Torr. Pressures were measured outside the gas cell, and an inside-outside pressure ratio of 800 was assumed, based on previous measurements.³ In the case of xenon, the maximum metastable current obtainable was 10^{-12} A, and the effective resolution was worse than 0.05 eV. The electron current entering the gas cell was about 10^{-7} A. Absolute cross sections were not measured because of imperfect knowledge of the incident current, target-gas pressure, and various geometric factors. The qualitative features of the excitation functions were unchanged over a wide range of pressures. The decrease in metastable currents from helium to xenon was mainly due to the decreasing threshold energy, since both incident current and metastable detection efficiency are decreased as the threshold lowers.

The circuitry associated with the electron spectrometer, as used in this experiment, is illustrated in Fig. 1. The monochromator was generally at a potential of 4 to 5 V, since this range gave the best combination of energy resolution and incident electron intensity. A stabilized electronic power supply E_0 was connected between the cathode and ground, and, since the gas cell

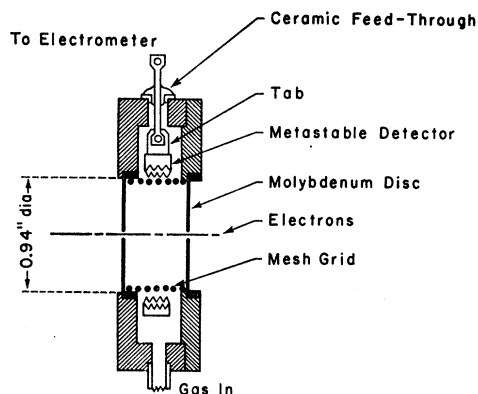


FIG. 2. Details of the gas cell.

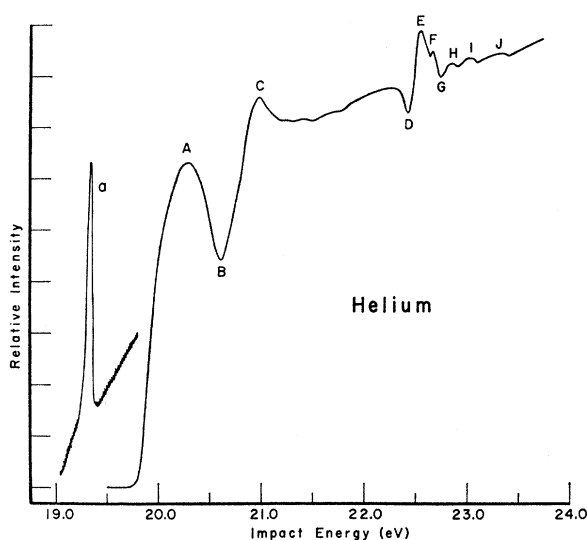


FIG. 3. Helium metastable current as a function of electron impact energy. Inset (a) shows the 19.3-eV elastic transmission resonance for helium plotted on the same voltage scale.

was grounded, this plus the contact potential between the cathode and target gas determined the impact energy. The contact potential of between 0.4 and 0.8 eV was such as to make the actual impact energy larger than E_0 . The amount of contact potential varied with the operating conditions of the gun, age of the tungsten cathode, and the type and pressure of the target gas. The impact energy was swept by placing a sawtooth generator in series with E_0 (switch position B in Fig. 1). The sawtooth generator also operated the X sweep of an XY recorder, and the metastable current was registered on the Y section of the recorder. The resultant plot gave, in arbitrary units, the total cross section for metastable excitation as a function of impact energy. It was assumed that the incident electron intensity and metastable detection efficiency were practically constant over the energy range swept. This assumption is discussed below when the results are examined in detail. Imperfect shielding of the metastable detector circuit within the vacuum system, together with the effect of leakage current due to the biasing, resulted in a noise level of about 5×10^{-13} A. The elastic transmission resonance in helium was measured on the same voltage scale as the metastable current to check the impact-energy calibration.

3. RESULTS AND DISCUSSION

A. Helium

A recorder trace of the excitation function for helium is shown in Fig. 3. The effective energy resolution was approximately 0.05 eV, as may be judged from the resonant structures near 22.5 eV and from the amount of curvature at the 19.8-eV threshold. Apart from occasional ripples, the noise level was barely above the width of the recorder trace. A curve with slightly higher

TABLE I. Measured energies (eV) of features in the excitation curve of helium (Fig. 4), and the nearby energy levels.

Curve (Fig. 4)	A	B	C	D	E	F	G	H	I	J
b	20.34	20.62	20.99	22.44	22.55	22.67	22.75	22.86	23.05	23.39
c	20.27	20.62	20.95							
d				22.35	22.43	22.53	22.60	22.70		
e				22.32	22.45	22.53	22.65	22.85	23.03	
f				22.38		22.61				
Helium energy levels										
2^3S	2^1S	2^3P	2^1P	3^3S	3^1S	3^3P	3^1P	$3^3D, 3^1D$	4^3S	4^1S
19.82	20.61	20.96	21.21	22.71	22.91	23.00	23.08	23.07	23.59	23.67

resolution was obtained with a monochromator voltage of about 3 eV. The incident electron intensity was an order of magnitude lower than was obtained for the trace of Fig. 3, and the noise level was proportionally higher. No new structural features were revealed by this trace.

Curve (a) in Fig. 3 is a sweep of the electron current transmitted through the gas cell and analyzer to the Faraday cup, and it shows the well-known 19.3-eV transmission resonance. This sweep was made without any change in the voltage scale, and served as a check on the energy calibration of the metastable excitation.

The threshold was measured by extrapolating the linear portions of the excitation and base lines to their point of intersection. The separation between this point and the peak of the transmission resonance was on the average (for the five best sets of data) 0.47 ± 0.03 eV. This compares with 0.51 ± 0.03 eV from the elastic-scattering data of Kuyatt *et al.*⁷ The 0.04-eV discrepancy, although within the combined quoted uncertainties, may be systematic. The effects of the energy spread in the incident beam, and of the energy

dispersion due to the Doppler effect (0.03 eV for helium at room temperature), may cause systematic shifts in the apparent thresholds.

The structural features of the excitation curve in Fig. 3 have been marked A–J. Their positions on the voltage scale were measured from the five best traces, and the mean results are presented in Table I. Most of the features were reproducible to within 0.02 eV. The values given in Table I are based on a calibration which sets the apparent threshold at the accepted value of 19.82 eV.⁹

In Fig. 4, our excitation curve (b) is compared with the data of Schulz and Fox¹⁰ (c); Schulz and Philbrick¹ (d); and Chamberlain³ (e and f). The set of points (c) were measurements of metastable excitation using the retarded-potential-difference (RPD) technique. It can be seen that our data (b) correspond closely in relative magnitude with the RPD data (c) throughout the energy range of interest. We assumed, therefore, that our incident electron intensity was practically independent of impact energy over this range, i.e., the change in potential between the monochromator and the gas cell produced a negligible defocusing effect. This independence of energy was achieved to some extent by adjusting the gun, deflecting plates (D_1, D_2 in Fig. 1), and einzel lens (L_1) to maximize the current incident at the threshold energy. The defocusing of the beam as the energy was swept upwards from threshold was thereby partly offset by the increasing transmission of the monochromator system.

The energies of features A, B, and C from curves (b) and (c) agree quite well (Table I), as do the extrapolated thresholds, despite the difference in the effective energy resolution. A comparison of the structures near 22.5 eV was not possible, since features D–G were not resolved in (c).

Curve (d) is proportional to the differential cross section for 2^3S excitation at a 72° scattering angle. Curves (e) and (f) are similar plots for a 0° scattering angle in the excitation of 2^1S and 2^3S , respectively. For convenience in plotting, curve (f) has been reduced in vertical scale by a factor of 3 relative to (e). There is no

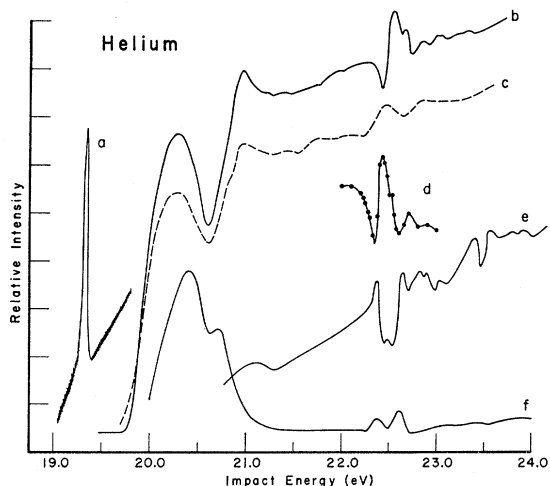


FIG. 4. A comparison of various experimental cross sections for helium plotted as a function of electron impact energy: (a) 19.3-eV elastic transmission resonance; (b) total metastable cross section (present work); (c) total metastable cross section (RPD method, Ref. 10); (d) 2^3S differential cross section at 72° (Ref. 1); (e) 2^1S differential cross section at 0° (Ref. 3); (f) 2^3S differential cross section at 0° (Ref. 3).

⁹ C. E. Moore, *Atomic Energy Levels*, Natl. Bur. Std. Circ. No. 467, Vol. I (1949); Vol. II (1952); Vol. III (1958).

¹⁰ G. J. Schulz and R. E. Fox, *Phys. Rev.* **106**, 1179 (1957).

TABLE II. Measured energies (eV) of features in the excitation curve of neon (Fig. 5), and the nearby energy levels.

Thresh. (calc.)	A	B	C	D	E	F	G	H	I	J
16.62	16.92	18.35	18.43	18.58	18.66	18.86	18.97	19.69	19.83	20.10
	Neon energy levels									
Config.	$2p^53S$	$2p^53p$	$2p^54S$	$2p^53d$	$2p^54p$	$2p^55S$	$2p^54d$			
Energy range	16.62-16.84	18.38-18.96	19.66-19.78	20.02-20.13	20.14-20.36	20.56-20.66	20.70-20.80			

relationship in vertical scale between any of the other curves in Fig. 4.

The shape of the structures $D-G$ in our data (b) and in the 72° energy-loss data (c) are strikingly similar. DE has the appearance of a resonance which dips below center, and rises above center (positive q).¹¹ In the $2^1S, 0^\circ$ data (e), this resonance seems to have q negative, and it appears to be symmetric ($q \sim 0$) in the $2^3S, 0^\circ$ data (f). In (b) and (c), FG possibly represents a resonance with negative q , and corresponds to the positive q resonance in (e) and the second $q \sim 0$ resonance in (f). Under these assumptions, we have compared the apparent energies of these resonances for (b), (d), (e), and (f) in Table I. The apparent positions of these two resonances vary somewhat in the different sets of data. These discrepancies probably arise from differing calibrations. The observed widths of these resonances are approximately 0.1 eV, somewhat larger than the limitations imposed by instrumental resolution and Doppler

broadening. The resonances $H, I,$ and J are too small for any discussion of their shape to be meaningful.

Recent work by Ehrhardt and Willmann¹² on the 2^3S differential cross sections at various angles has indicated the presence of a resonance very close to threshold (about 20.1 eV). This resonance, which predominates at angles larger than 30° , has an apparent width of 0.15 eV, and should be well within the energy-resolving capabilities of our apparatus. We have made a careful examination of the threshold region of the metastable current, and have failed to observe any indication of structure near 20.1 eV, and therefore suggest that this resonance does not appear in the total cross section.

B. Neon

Figure 5, curve (a), is the excitation function (about 0.05-eV resolution) taken for the $(2p^53s) [1\frac{1}{2}]^\circ (J=2)$ and $(2p^53s) [\frac{1}{2}]^\circ (J=0)$ metastable states of neon. Inset (b) is a detail of the 18-19-eV region which was taken at

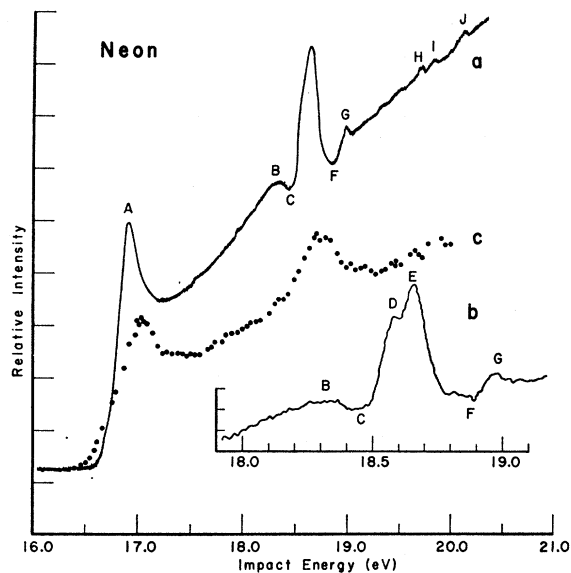


FIG. 5. Total metastable cross sections for neon plotted as a function of electron impact energy: (a) present work, 0.050-eV resolution; (b) detail of 18-19-eV region, 0.035-eV resolution; (c) RPD method (Ref. 5).

¹¹ U. Fano, Phys. Rev. **124**, 1866 (1961); U. Fano and J. W. Cooper, *ibid.* **137**, A1364 (1965). The parameter q is defined so that the cross section near resonance has the functional form $\sigma(\epsilon) = \sigma_a(q + \epsilon)^2 / (1 + \epsilon^2) + \sigma_b$, where $\epsilon = (E - E_r) / 0.5\Gamma$, E is the electron energy, E_r is the energy at the resonance center, Γ is the resonance width, and σ_a and σ_b are, respectively, the components of the cross section which are and are not affected by the resonance.

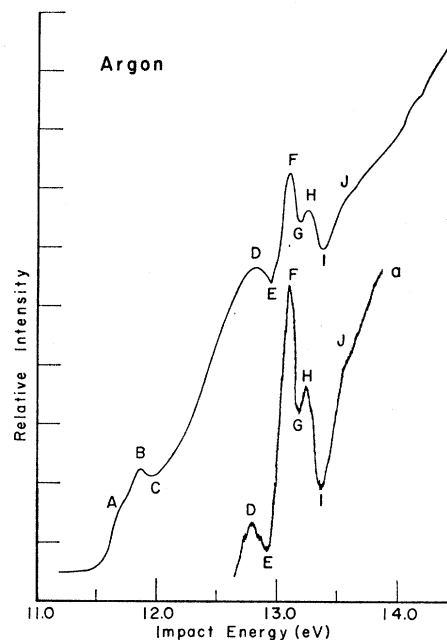


FIG. 6. Total metastable cross section for argon plotted as a function of electron impact energy. Inset (a) shows the region between 12.6 and 14.0 eV on a more sensitive vertical scale.

¹² H. Ehrhardt and K. Willmann, in *Proceedings of the Fifth International Conference on the Physics of Electronic and Atomic Collisions, Leningrad, USSR, 1967* (Nauka, Leningrad, 1967), p. 486.

TABLE III. Measured energies (eV) of features in the excitation curve of argon (Fig. 6), and the nearby energy levels.

Thresh. (calc.)	A	B	C	D	E	F	G	H	I	J
11.55	11.72	11.88	11.98	12.80	12.93	13.08	13.17	13.24	13.37	13.55
	Argon energy levels									
Config.	$3p^54s$		$3p^54p$		$3p^53d$		$3p^55s$		$3p^55p$	
Energy range	11.55–11.83		12.90–13.48		13.84–14.30		14.06–14.25		14.46–14.73	
									$3p^54d$	
									14.69–15.00	

higher resolution (about 0.035 eV), showing partial resolution of the structures C–F. The energy scale has been calibrated by extrapolating the threshold and setting it at the accepted value⁹ of 16.615 eV for the above ($J=2$) state.

The average measured energies for structures A–I are presented in Table II. The principal structures were reproducible to 0.02 eV. The two predominant resonances near 18.6 eV, C–D and E–F, apparently have positive and negative q 's, respectively, and these are in the energy region of the ($2p^53p$) configuration of the target atom (Table II).

The resonance A near threshold is relatively sharp (compare the corresponding resonance in helium). The apparent width of 0.15 eV remained sensibly constant when a similar curve was taken at 0.035-eV resolution, and no new structure was revealed.

The set of points (c) in Fig. 5 are the data of Olmsted *et al.*⁵ using the RPD technique. It can be seen that the

lower resolution in the RPD data affects the slope of the curve just above threshold, and shifts the apparent position of resonance A. The RPD technique has also been used by Dowell,¹³ who obtained results similar to those of Olmsted *et al.*, with improved signal-to-noise ratios and energy resolution. Peaks D, E, and G were not resolved.

C. Argon

Figure 6 shows the excitation curve for argon taken with a resolution of about 0.05 eV. The energy scale has been calibrated from the assumed 11.55-eV threshold for the ($3p^54s$) [$1\frac{1}{2}$]^o ($J=2$) metastable state. The other metastable state is ($3p^54s$) [$\frac{1}{2}$]^o ($J=0$) with a threshold at 11.72 eV, and there is a definite break in the curve (feature A) at this point.

The region near 13.0 eV is shown at higher sensitivity in inset (a), Fig. 6. DEF appears to be a sharp, $q\sim 0$ resonance, and it is not fully resolved from GHI, which could be a $q\sim 0$ resonance. Another resonance is apparent at the change in slope J.

The critical effect of the energy resolution on the nature of the excitation curves is illustrated in Fig. 7 with curves of resolutions 0.15, 0.10, and 0.05 eV, together with the point-by-point RPD data of Olmsted

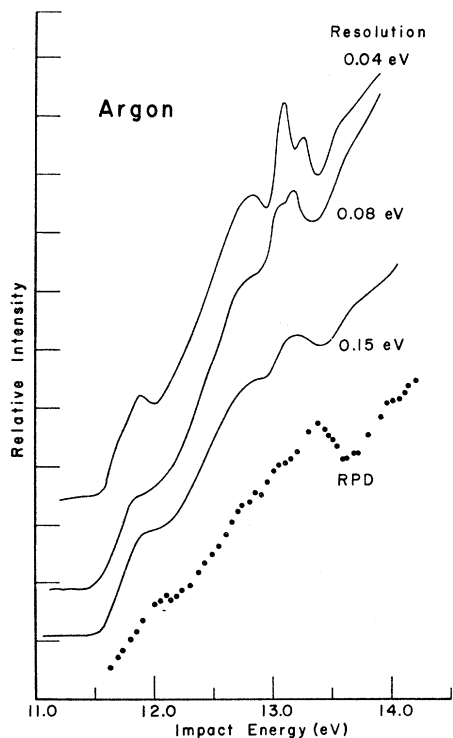


FIG. 7. Total metastable cross sections for argon plotted as a function of electron impact energy observed with electron energy resolutions of 0.04, 0.08, and 0.15 eV (present work) compared with results obtained using the RPD technique (Ref. 5).

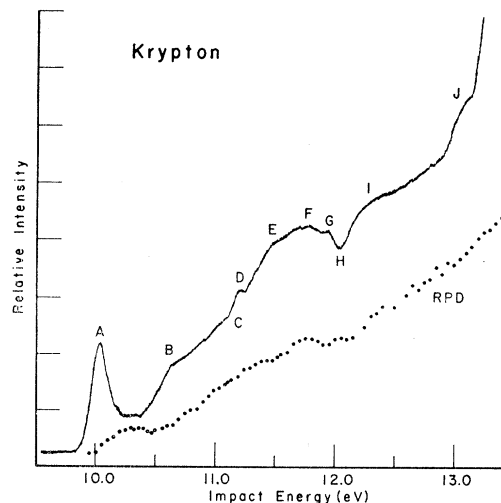


FIG. 8. Total metastable cross section for krypton plotted as a function of electron impact energy. Dotted curve was obtained using the RPD technique (Ref. 5).

¹³ J. T. Dowell, thesis, University of California at Livermore, 1965, University of California Radiation Laboratory Report No. UCRL-14 450 (unpublished).

TABLE IV. Measured energies (eV) of features in the excitation curve of krypton (Fig. 8), and the nearby energy levels.

Thresh. (calc.)	A	B	C	D	E	F	G	H	I	J
9.91	10.05	10.63	11.10	11.20	11.48	11.70	11.94	12.04	12.28	13.08
	Krypton energy levels									
Config.	$4p^55s$	$4p^55p$	$4p^54d$	$4p^56s$	$4p^56p$	$4p^55d$	$4p^57s$			
Energy range	9.91-10.64	11.30-12.25	12.00-13.00	12.35-13.03	12.75-13.49	12.90-13.73	13.10-13.76			

*et al.*⁵ It can be seen that the apparent positions of multiple structures such as *D-I* are quite critically dependent on the effective resolution of the apparatus. The energy calibration of the RPD data may differ by some 0.15 eV from ours.

B may be a very sharp resonance which has been resolved only partially; the 0.10-eV resolution curve (Fig. 7) shows no indication of the minimum. In fact, there may be a multiple structure starting with *AB* as a $q \sim 0$ resonance, and complicated by the fact that *A* coincides with the ($J=0$) metastable threshold.

The positions of the various structures are summarized in Table III.

D. Krypton

The excitation curve for krypton is shown in Fig. 8, together with the RPD data of Olmsted *et al.*⁵ Our resolution was probably somewhat better than 0.05 eV, and we calibrated the energy scale from the assumed 9.91-eV threshold⁹ of the ($4p^55s$) [$1\frac{1}{2}$]^o ($J=2$) metastable state. The threshold of the other metastable state ($4p^55s$) [$\frac{1}{2}$]^o ($J=0$) is at 10.56 eV, very close to feature *B* (10.63 eV).

The resonance *A* just above threshold is very sharp, and actually masks the broader 10.35-eV peak in the RPD data. This effect is illustrated in Fig. 9, where we show the threshold region taken at different energy resolutions, together with the RPD data. The energy calibration of the RPD data may be somewhat different.

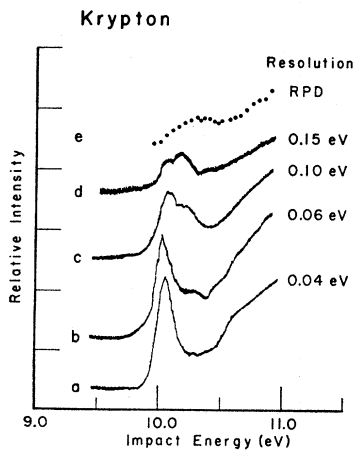


FIG. 9. The threshold region of the krypton metastable cross section observed with electron energy resolutions of 0.04, 0.06, 0.10, and 0.15 eV (present work) compared with results obtained using the RPD technique (Ref. 5).

It can be seen that peak *A* rises dramatically as the resolution is increased, and is probably not even fully resolved in curve (a), Fig. 9. The second broader peak is more clearly seen in curves (b), (c), (d), and its apparent position seems to depend on the experimental resolution.

The resonance *CD* (Fig. 8) probably has $q > 0$. It only appeared in the high-resolution curves, and is unfortunately situated in a region of rising background. The changes in slope *E*, *F*, and *I*, although small, were clearly reproducible. *GH* may be a $q < 0$ resonance complicated by *H* being also part of a broader minimum.

An interesting feature is the sudden rise at 13.15 eV. This is not reproduced in the RPD data, and is some 0.85 eV below the threshold for ionization. A possible explanation is that the current arises from electrons ejected in the de-excitation of optically excited states with large principal quantum numbers. The separation between our detector and the scattering region was 1.6 cm, compared with 22 cm in the RPD apparatus. This effect could then be explained by the excitation of states having radiative lifetimes somewhere between 1×10^{-5} and 5×10^{-4} sec.

The positions on our energy scale of the various features are summarized in Table IV.

E. Xenon

An excitation curve for xenon is shown in Fig. 10. The effective signal-to-noise ratio attainable with this target

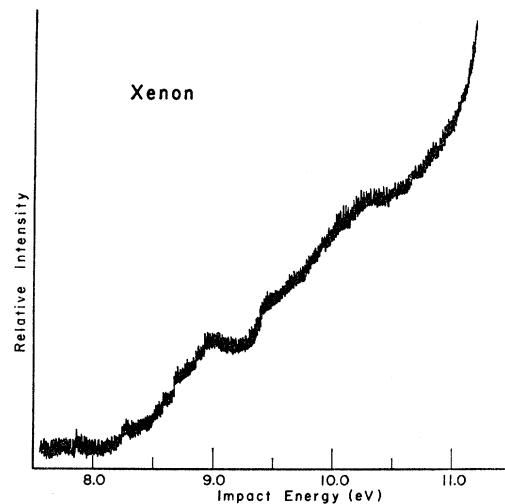


FIG. 10. Total metastable cross section for xenon plotted as a function of electron impact energy.

was so poor that only a broad peak at 9.0 eV and shoulders at 9.5 and 10.3 eV were distinguishable. There is a steep rise at 11.2 eV which, similar to the case of krypton, is some 0.9 eV below the ionization threshold.

ACKNOWLEDGMENTS

The authors are grateful to S. R. Mielczarek, Dr. G. E. Chamberlain, and Tully Pound for considerable as-

sistance and advice concerning the experimental apparatus; to Dr. C. E. Kuyatt and Dr. J. W. Cooper for several valuable comments and suggestions; and to Dr. K. G. Kessler for his interest and support. One of us (F.M.J.P.) would like to express his appreciation to the National Bureau of Standards for its hospitality, and to Yale University for a Junior Faculty Fellowship which made possible his visit to the National Bureau of Standards.

Paramagnetic-Resonance Spectrum of Metastable (2D) Atomic Nitrogen*

H. E. RADFORD† AND K. M. EVENSON

National Bureau of Standards, Boulder, Colorado 80302

(Received 13 November 1967)

The paramagnetic-resonance spectrum of free metastable (2D) nitrogen atoms has been observed in the flowing products of an electric discharge in nitrogen-helium gas mixtures. An analysis of the Zeeman effect and hyperfine structure yields the following values for the atomic g factors and radial integrals: $g_J(^2D_{5/2}) = 1.20036 \pm 0.00001$; $g_J(^2D_{3/2}) = 0.79949 \pm 0.00002$; $\langle r_i^{-3} \rangle = (20.21 \pm 0.02) \times 10^{24} \text{ cm}^{-3}$; $\langle r_s^{-3} \rangle = (22.22 \pm 0.02) \times 10^{24} \text{ cm}^{-3}$. The 2D fine-structure separation is found to be $-8.69 \pm 0.02 \text{ cm}^{-1}$. Evidence is found of a small electric-quadrupole hyperfine-structure interaction.

INTRODUCTION

RECENT work at this laboratory has shown it possible to detect paramagnetic-resonance absorption by metastable (2D) nitrogen atoms in a mixture of nitrogen and helium gas that has passed through an electric discharge.¹ The spectrum is interesting because it shows well-developed anisotropic hyperfine structure, a type of hyperfine structure which the familiar spectrum^{2,3} of ground-state (4S) atomic nitrogen does not have, and also because it provides an alternative technique of studying the formation and decay of metastable nitrogen atoms, a technique with some potential advantages over those of optical^{4,5} and mass⁶ spectrometry. As first observed, the absorption lines were weak and broad, and subsequent efforts have been made to intensify and sharpen the 2D spectrum, and to detect the corresponding spectrum of the metastable 2P term. These efforts have not succeeded, and the present report is limited, therefore, to an analysis of the hyperfine structure and Zeeman effect of the 2D term, based on precise measurements of spectra like that of Fig. 1, which is reprinted here from the earlier report.

* Supported in part by the U. S. Office of Naval Research.

† Permanent address: National Bureau of Standards, Washington, D. C. 20234.

¹ K. M. Evenson and H. E. Radford, *Phys. Rev. Letters* **15**, 916 (1965).

² M. A. Heald and R. Beringer, *Phys. Rev.* **96**, 645 (1954).

³ K. M. Evenson and D. S. Burch, *J. Chem. Phys.* **45**, 2450 (1966).

⁴ J. F. Noxon, *J. Chem. Phys.* **36**, 926 (1962).

⁵ Y. Tanaka, A. S. Jursa, F. J. LeBlanc, and E. C. Y. Inn, *J. Planet. Space Sci.* **1**, 7 (1959).

⁶ S. N. Foner and R. L. Hudson, *J. Chem. Phys.* **37**, 1662 (1962).

EXPERIMENT

A double modulation (100-kHz and 100-Hz) X-band electron-paramagnetic-resonance (EPR) spectrometer was used to measure the spectra. In order to obtain the desired accuracy of one part in 10^5 , each $^2D_{3/2}$ line was traced 2 to 6 times with a 1-sec time constant, and each $^2D_{5/2}$ line was traced 6 to 12 times with a 3-sec time constant.

A standard frequency counter accurate to one part in 10^8 and a transfer oscillator were used to measure the klystron frequency. The same counter was used to measure (to about one part in 10^6) the resonant frequency of the nuclear-magnetic-resonance (NMR) magnetic-field probe, which contained a cylindrical sample of mineral oil 2 mm in diameter and 10 mm long. A small correction, typically $0.3 \pm 0.01 \text{ G}$ at 5500 G and $1.0 \pm 0.3 \text{ G}$ at 8300 G, was made for the difference between the magnetic field at the center of the EPR cavity and the NMR-probe position. The difference was due partly to the field inhomogeneity of the electromagnet and partly to a paramagnetic impurity in the material from which the EPR cavity was constructed. The klystron frequency was locked to the cavity resonance, and was monitored continuously during the recording of each EPR line; the uncertainty in measuring this frequency was one part in 10^6 , due to small drifts of the klystron frequency during the sweeping of each line. The largest inaccuracy in the measurements was in determining the exact center of each line; in the weakest of the lines a single scan yielded the line center to about 3 parts in 10^5 . However, 10 or more